TRIB2 regulates the expression of miR-33a-5p through the ERK/c-Fos pathway to affect the imatinib resistance of chronic myeloid leukemia cells

HANG SUN[1,2*], YOUJIE LI[2*], XIAO WANG[2*], XUE ZHOU[1], SIMIN RONG[2], DONGMIN LIANG[2], GUANGBIN SUN[2], HUIZHEN CAO[1], HONGFANG SUN[2], RANRAN WANG[3], YUNFEI YAN[2], SHUYANG XIE[2] and YUNXIAO SUN[1]

[1]Department of Pediatrics, Yantai Affiliated Hospital of Binzhou Medical University, Yantai, Shandong 264100; [2]Department of Biochemistry and Molecular Biology; [3]School of Rehabilitation Medicine, Binzhou Medical University, Yantai, Shandong 264033, P.R. China

Received November 30, 2021; Accepted February 15, 2022

DOI: 10.3892/ijo.2022.5339

Abstract. Chronic myeloid leukemia (CML) is a hematological disease, and imatinib (IM) resistance represents a major problem for its clinical treatment. In the present study, the role of tribbles pseudokinase 2 (TRIB2) in IM resistance of CML and the possible mechanism were investigated. It was found that TRIB2 was highly expressed in IM-resistant patients with CML through the Oncomine database and this conclusion was confirmed using reverse transcription-quantitative PCR and western blot experiments. Knockdown of TRIB2 was found to increase the drug sensitivity of KG cells to IM using Cell-Counting Kit-8 (CCK-8) assays, and the low-expression TRIB2 mice were further found to be more sensitive to the IM and have a higher survival rate in leukemia model mice. Moreover, using western blot and luciferase experiments, it was found that TRIB2 could regulate c-Fos through the ERK signaling pathway, and c-Fos suppressed the transcriptional activity and the expression of miR-33a-5p. Further investigation identified that the binding site for c-Fos to function on miR-33a-5p was the -958-965 region. Finally, CCK-8 assays and western blot experiments demonstrated that miR-33a-5p could inhibit the proliferation of KG cells and reduce IM resistance by suppressing the expression of HMGA2. In conclusion, it was demonstrated that TRIB2 regulates miR-33a-5p to reverse IM resistance in CML, which may help identify novel targets and therapeutic strategies for the clinical treatment of IM resistance.

Correspondence to: Professor Yunxiao Sun, Department of Pediatrics, Yantai Affiliated Hospital of Binzhou Medical University, 717 Jinbu Street, Yantai, Shandong 264100, P.R. China
E-mail: sunyunxiao1979@163.com

Professor Shuyang Xie, Department of Biochemistry and Molecular Biology, Binzhou Medical University, 346 Guanhai Road, Yantai, Shandong 264033, P.R. China
E-mail: shuyangxie@aliyun.com

*Contributed equally

Key words: tribbles pseudokinase 2, chronic myeloid leukemia, c-Fos, imatinib-resistance, microRNA-33a-5p

Introduction

Chronic myeloid leukemia (CML), which is a malignant myeloproliferative disorder caused by hematopoietic stem cells (HSCs), is a clonal disorder of HSCs (1,2). Various treatments are available for patients with CML, including tyrosine kinase inhibitors (TKIs), HSC transplantation and chemotherapy (3). Imatinib (IM) is a targeted agent after clinical experiments that has become an established treatment for CML, and was first approved as a first-line drug in 2003 (4,5). IM is a TKI that has revolutionized the treatment of CML, and a large amount of clinical data have shown that this drug can induce complete remission of CML and change the clinical course (6,7). However, finding an effective treatment for IM-resistant patients remains challenging despite the progress and success of IM in CML treatment. Drug resistance is undoubtedly emerging as a major problem in the treatment of CML. Thus, finding ways and mechanisms to tackle tumor drug resistance is urgent. In the present study, the K562 CML cell line and its IM-resistant cell line (KG) were used to investigate the mechanism underlying CML resistance to IM and to identify potential strategies to reverse resistance.

Tribbles pseudokinase 2 (TRIB2) is a member of the tribbles family (8). TRIB2 includes an N-terminal domain, a C-terminal domain and a central pseudokinase domain. Under the absence of kinase activity, it can regulate different signaling pathways in basic biological processes and pathology. For instance, TRIB2 blocks cellular senescence through AP4/p21 signaling and can also regulate the differentiation of myeloid progenitors transduced with mll-tet1 (9,10). TRIB2 plays an important role in regulating tumor cell proliferation, apoptosis and drug resistance (11,12). TRIB2 acts as a tumor promoting factor and plays a promoting role in tumorigenesis and development. Link *et al* (13) have

reported that TRIB2 suppresses FOXO and acts as an oncogenic protein in melanoma. TRIB2 also plays a tremendous role in tumor cell drug resistance. Wang *et al* (14) found that combined elevation of TRIB2 and MAP3K1 indicates poor prognosis and chemoresistance to temozolomide in glioblastoma. Meanwhile, Hill *et al* (15) reported that TRIB2 confers resistance to anti-cancer therapy by activating the serine/threonine protein kinase AKT. Therefore, investigating the role played by TRIB2 in tumor drug resistance is urgent and meaningful. The present study investigated the relationship between TRIB2 and IM resistance in CML and identified that reversal of CML resistance was through regulation of miR-33a-5p.

MicroRNAs (miRNAs) are a family of small non-coding RNAs consisting of 18-25 nucleotides (16). miRNA plays important roles in numerous cellular and biological processes, such as proliferation, apoptosis, differentiation and metabolism (17). Concurrently, a largely relationship exists between miRNA and drug resistance of tumor cells (18). Diaz-Martinez *et al* (19) found that miR-204-5p and miR-211-5p contribute to melanoma resistance against BRAF inhibitors. In addition, exosomal transfer of miR-1238 contributes to temozolomide resistance in glioblastoma (20). Thus, miRNA plays an important role in reversing tumor drug resistance. Thus, in the present experiment, the function of miR-33a-5p in CML-resistant cells was investigated. Although miRNA expression plays an important role in tumorigenesis and drug resistance, little is known about the mechanisms leading to aberrant miRNA regulation in cancer. Numerous upstream factors affect miRNAs, including proteins that exercise various functions and non-coding RNAs (21,22). Meanwhile, transcription factors (TFs) are the most intensely studied factors. The role played by TFs in regulating miRNAs needs to be further explored.

TFs are key regulators controlling gene expression in the process of carcinogenesis and development (23). C-Fos is a well-known oncogene and a member of AP-1 TF family (24). It can be used as a TF to regulate the development of tumor cells. C-myc is a major transcriptional regulator of RhoA, and alkaline phosphatase downregulation promotes lung adenocarcinoma metastasis via the c-myc/RhoA axis (25). C-Fos was predicted as a possible TF of miR-33a-5p using *in silico* bioinformatics analysis (http://alggen.lsi.upc.es/cgi-bin/promo_v3/promo/promoinit.cgi?dirDB=TF_8.3).

Similar to c-myc/RhoA, the mechanism by which c-Fos acts as a TF to affect miR-33a-5p remains to be investigated. Increasing clinical and biological evidence indicated that the ERK pathway plays a key role in the progression of tumors (26). The mechanism of ERK pathway involvement in the present study was investigated using ERK signaling pathway blockers and activators. The specific mechanism through which TRIB2 may reverse the IM resistance process of CML cells by regulating miR-33a-5p was investigated. The present study provided a new therapeutic target for CML treatment and acquired resistance to IM and a new strategy for clinical treatment.

Materials and methods

Cell culture and reagents. The cell line K562 was kindly provided by the Cell Bank of The Chinese Academy of Sciences (Shanghai, China). IM (Aladdin Industrial Corporation) was added to the logarithmic growth phase K562 cell suspension at a final concentration of 100 ng/ml. The cells were observed so that the drug dose could be gradually escalated over the time of incubation and the cells were finally allowed to survive on a concentration of 10 μM IM in the culture system. Monoclonal screening by limiting dilution yielded an IM resistant KG cell line. The cells were incubated in basic RPMI-1640 medium with 10% fetal bovine serum (both from Gibco; Thermo Fisher Scientific, Inc.) and 1% penicillin-streptomycin (Beyotime Institute of Biotechnology) at 37˚C in a 5% CO_2 humidified atmosphere. KG cells were maintained in the presence of 10 μM IM. Prior to the experiment, the cells were cultured in drug-free medium for 2 weeks. All cell experiments were repeated three times. Honokiol (HNK) was purchased from Aladdin Industrial Corporation, and U0126 was obtained from Promega Corporation. At 50-60% of KG cells, 20 μM U0126 or 20 μM HNK at 37˚C for 24 h for subsequent experiments.

Cell viability assay. Cell viability was determined by Cell Counting Kit-8 (CCK-8) assays. Briefly, the cells were grouped and treated differently. Then, KG cells were seeded in 96-well plates ($4x10^3$ cells/well) and cultured in an incubator at 37˚C with 5% CO_2. A volume of 10 μl CCK-8 (Beyotime Institute of Biotechnology) was added into the wells for 2 h at 0, 24, 48 and 72 h. The absorbance of each well at 450 nm (A450) wavelength was measured by a microplate reader (Multiskan FC; Thermo Fisher Scientific, Inc.). The IM resistance index was calculated as IC_{50}-KG/IC_{50}-K562; i.e., drug resistance index=IC_{50} of drug resistant cells/IC_{50} of parental cells. In the present study that was IC50-KG/IC50-K562=24.12/0.98=24.61.

Cell infection. The KG cells were routinely cultured in six-well plates. A total of 12 μg lentiviral expression vectors (pCDH-NC or pCDH-TRIB2; KeyyBio Scientific, Inc.) and second-generation lentiviral packaging vectors pSPAX2 and pMD2.G (from Addgene) were transfected into 293T (Shanghai Cell Bank of the Chinese Academy of Sciences, Shanghai, China) cells at a ratio of 4:3:2 and cultured at 37˚C. The virus was three times collected at an interval of 24 h between collections. KG cells were infected using polybrene (Sigma) and lentiviral particles at an MOI of 20. KG cells were seeded within six well plates and cultured in a 37˚C 5% CO_2 incubator until transfection was performed at a cell density of 50-60%. GV141-Fos (2 μg) and 6 μl Lipofectamine 2000® reagent (Invitrogen; Thermo Fisher Scientific, Inc.) were added at the time of transfection and empty plasmid served as a negative control. Fluid changes were performed after 6-8 and 48 h for subsequent experiments.

Negative control siRNA was used as a negative control (NC). The sequences were as follows: si-NC sense, 5'-UUCUCCGAACGUGUCACGUTT-3' and si-NC antisense, 5'-ACGUGACACGUUCGGAGAATT-3'; si-TRIB2 sense, 5'-UAGCGAGAUAUGGGAGAUCTT-3' and si-TRIB2 antisense, 5'-GAUCUCCCAUAUCUCGCUATT-3'. The sequences of the miR-33a-5p-mimics were as follows: sense, 5'-GUGCAUUGUAGUUGCAUUGCA-3' and antisense, 5'-UGCAAUGCAACUACAAUGCACUU-3'. The sequences of the miR-33a-5p-NC were as follows: sense, 5'-CAGUACUUUUGUGUAGUACAA-3' and antisense,

Table I. Primer sequences.

Vector name	Primer sequences (5'→3')
-2000 ~ +69 nt	F: CTAGCTAGCCAAGTTGGGCCAGCAG
	R: CCCAAGCTTCTGTGATGCACTGTGGAA
-1575 ~ +69 nt	F: CTAGCTAGCTGATGGGCAGCCCTG
	R: CCCAAGCTTCTGTGATGCACTGTGGAA
-1124 ~ +69 nt	F: CTAGCTAGCCCTGCAGGCACTGCT
	R: CCCAAGCTTCTGTGATGCACTGTGGAA
-534 ~ +69 nt	F: CTAGCTAGCCCCTGGGAAAGCAGATG
	R: CCCAAGCTTCTGTGATGCACTGTGGAA
Mutation (A)	F: GGAATGATGTCGACACGTTGGAATGA
	R: TTACCTATAAAGTGGCCACAATAAGGT
Mutation (B)	F: GCACCACTGGATTAGTGACCTGCCTCT
	R: GTGACAGGCAGAGGGGCCCAAGCCA

F, forward; R, reverse.

5'-GUACUACACAAAAGUACUGUU-3'. The sequences of the miR-33a-5p-inhibitor were as follows: 5'-UGCAAUGCA ACUACAAUGCACUU-3'. After 24 h, the changes in GFP expression were detected by fluorescence microscopy and flow cytometry and images were captured. After 48 h, G418 (300 μg/ml) was used to select and maintain stably transfected cells. After 4 weeks, the cells expressing GFP were selected using a BD FACSAria II flow cytometer (BD FACSAria II; BD Biosciences) to obtain a stably transfected cell line.

Vector construction. The possible binding sites of c-Fos in the promoter of miR-33a-5p were analyzed using JASPAR (http://jaspardev.genereg.net/). All miR-33a-5p promoter sequences were segmented according to c-Fos binding sites (-534 ~+69 nt, -1124 ~+69 nt, -1575 ~+69 nt, and -2,000 ~+69 nt), and they were connected to pGL3 basic luciferase reporter gene vector (Promega Corporation) to construct promoter luciferase segmented vector. The promoter binding site was point-mutated, amplified by PCR and cloned into pGL3 basic luciferase reporter gene vector to construct luciferase mutation vector. PCR amplification was performed using a Takara LA Taq DNA polymerase (Takara Biotechnology Co., Ltd.). The PCR conditions were as follows: initial denaturation at 94˚C for 1 min; 30 cycles of 94˚C for 30 sec, 60˚C annealing for 30 sec and extension at 72˚C for 2 min. The amplification was completed with a final step of 72˚C for 5 min. PCR products were separated by electrophoresis on a 1.25% agarose gel followed by visualization under the Tanon 2500 gel imaging system (Tanon Science and Technology Co., Ltd.). A pair of primers was designed on both ends of the miR-33a-5p promoter truncation fragments based on their size and location (i.e., -534, -1,124, -1,575 and -2,000). A protective base and a specific enzymatic cleavage site before the primer sequence were added. The primer sequences are listed in Table I.

Luciferase activity assay. Cancer cells ($6x10^3$/well) were seeded in six-well plates and luciferase vectors containing the miR-33a-5p promoter (miR-33a-5p-luc) were co-transfected with TRIB2 and c-Fos expression vectors using Lipofectamine® 2000 reagent (Invitrogen; Thermo Fisher Scientific, Inc.). After 48 h of transfection, the cells were collected and lysed on ice. The luciferase activity was detected according to the manufacturer's instructions using a double luciferase detection kit (Promega Corporation). Firefly luciferase activity was normalized to *Renilla* luciferase activity. Targetscan7.1 (http://www.targetscan.org/vert_71/) was used to predict the downstream target genes of miR-33a-5p.

Western blot analysis and immunoprecipitation. Differently treated KG cells were collected, washed twice with cold PBS and lysed on ice in RIPA lysis buffer (Beyotime Institute of Biotechnology) for 30 min. The BCA method was used to determine protein concentration, and 20 μg protein were loaded per lane. Proteins were separated using 10% SDS-PAGE and transferred to a PVDF membrane. The membrane was blocked in 5% milk powder for 2 h at 37˚C. The membrane was incubated with primary antibodies at 4˚C overnight. The next day, the membrane was washed with TBST (0.1% Tween-20) three times and incubated with goat anti-rabbit IgG (H+L) HRP conjugate (1:5,000; cat. no. BS13278; Bioworld Technology, Inc.) for 2 h at 4˚C and detected by chemiluminescence (ECL reagent; Biosharp Life Sciences) method. The densities of the bands were analyzed using iBright 1500 v1.4.3 software (Thermo Fisher Scientific, Inc.) The information for antibodies are as follows: TRIB2 (1:1,000; cat. no. ab272544; Abcam), c-Fos (1:500; cat. no. 48283; SAB Technology, Inc.), p-c-Fos (1:750; cat. no. 12599; SAB Technology, Inc.), ERK (1:750; cat. no. BS1112; Bioworld Technology, Inc.), p-ERK (1:500; cat. no. BS65784; Bioworld Technology, Inc.) and GAPDH (1:10,000; cat. no. BS65483M; Bioworld Technology, Inc.). For immunoprecipitation, the cells were lysed on ice with NP-40 lysis buffer (Beyotime Institute of Biotechnology) for 30 min and total cell lysates were incubated with appropriate antibodies overnight at 4˚C and subsequently rotated with protein A/G beads (50 μl; cat. no. 20421; Thermo Fisher Scientific, Inc.) for 4 h at 4˚C. The information for antibodies are as

follows: IgG (1:5,000; cat. no. ab181236; Abcam), p-c-Fos (1:100; cat. no. 5348; Cell Signaling Technology), TBP (1:100; cat. no. 44059; Cell Signaling Technology). Beads were washed three times using NP-40 lysis buffer, mixed with 2X SDS sample buffer and boiled for 10 min. The co-precipitates were analyzed by western blot analysis.

Chromatin immunoprecipitation (ChIP) assay. ChIP assay was performed using a ChIP assay kit (Beyotime Institute of Biotechnology). Briefly, differently treated KG cells were collected and treated with 1% formaldehyde for 10 min at 37˚C for cross-linking. Chromatin was sheared by sonication on ice to produce DNA fragments with a size of 200-1,000 bp. Chromatin was immunoprecipitated with 5 μg of anti-p-c-Fos (1:100; cat. no. 5348; Cell Signaling Technology) or rabbit IgG (1:5,000; cat. no. ab181236; Abcam). The immunoprecipitated DNA was amplified with a primer pair specific for the miR-33a-5p promoter (forward, 5'-CCTGCAGGCACT GCT-3' and reverse, 5'-CTGTGATGCACTGTGGAA-3'). PCR amplification was performed using a TaKaRa LA Taq DNA polymerase (Takara Biotechnology Co., Ltd.). The PCR conditions were as follows: initial denaturation at 94˚C for 1 min; 35 cycles of 95˚C for 20 sec, 60˚C annealing for 30 sec and extension at 72˚C for 2 min. The amplification was completed with a final step of 72˚C for 3 min.

Reverse transcription-quantitative (RT-q) PCR. KG cells transfected with TRIB2 and miR-33a-5p expression vectors were collected and RNA was extracted using TRIzol® reagent (Thermo Fisher Scientific, Inc.). Reverse transcription of RNA was performed to generate cDNA using PrimeScript RT reagent kit with gDNA Eraser (Takara Bio, Inc.) according to the manufacturer's protocol. Reaction system was determined through RT-qPCR by employing the 7500 Real-Time PCR System using TB Green (Takara Biotechnology Co., Ltd.). The qPCR conditions were as follows: initial denaturation at 95˚C for 30 sec; 40 cycles of 95˚C for 10 sec, 60˚C annealing for 20 sec and extension at 72˚C for 20 sec. The $2^{-\Delta\Delta Cq}$ method was used to calculate relative expression and fold change. Primers were purchased from Guangzhou RiboBio Co., Ltd. The sequences of the primers were as follows: TRIB2 forward, 5'-CTCCGAACTTGTCGCATTG-3' and reverse, 5'-CACATA GGCTTTGGTCTCAC-3'; GAPDH forward, 5'-GACAGT CAGCCGCATCTTCTT-3' and reverse, 5'-AATCCGTTGACT CCGACCTTC-3'; miR-33a-5p forward, 5'-GTGCATTGTAGT TGCATT-3' and reverse, 5'-AACATGTACAGTCCATGG ATG-3'; and 5s rRNA forward, 5'-GCCATACCACCCTGA ACG-3' and reverse, 5'-AACATGTACAGTCCATGGATG-3'. GAPDH and 5S rRNA were used as the reference genes.

Animal model. The animal experiments were reviewed and approved (approval no. 2019-11-06) by the ethics committee of Binzhou Medical University (Yantai, China). Cell lines were injected subcutaneously into the armpits of approximately 20 g female nude mice at 4-5 weeks of age. A total of five mice were injected for each group of cells. They were kept in a laminar airflow cabinet under specific pathogen-free conditions with a controlled temperature (23±2˚C), humidity (40-70%) with free access to food and water. The number of injected cells was $5x10^6$. Cells were resuspended with PBS. Mice were anesthetized with 50 mg/kg sodium pentobarbital. A total of 70 μl cells and 30 μl Matrigel (BD Biosciences) mixed together were injected subcutaneously into nude mice. When the tumors became visible to naked eyes after ~a week, tumor volume was calculated every 4 days and a tumor growth curve was plotted. Finally, the mice were anesthetized by inhalation of 3% isoflurane and sacrificed by cervical dislocation. The mice were euthanized on day 28 after cancer cell injection. The weight of tumors was then measured and the results were analyzed.

KG cells stably transfected with TRIB2, NC and si-TRIB2 were directly inoculated into the NOD scid gamma (NSG) mice caudal vein. A total of four mice were injected for each group of cells. The number of injected cells was $2x10^6/100$ μl. Peripheral blood was collected from the tail vein regularly for blood cell count and blood smear observation in order to monitor the successful establishment of the model. After successful modeling, one group was treated with 50 mg/kg IM and one with 0.9% normal saline.

Determination of blood parameters. One week after constructing leukemia model mice, mice were subjected to tail cutting for blood collection. The blood was collected in EP tubes containing EDTA-K2 anticoagulant for upper machine analysis within 4 h. Blood cell counts and classification were determined with a fully automated blood cell analyzer (Hemavet®950, Drew Scientific, Inc.).

Statistical analysis. Normality tests were conducted on all data with Shapiro-Wilk test, and all data were assessed for normality of distribution. All experimental data are expressed as the mean ± standard deviation (mean ± SD). Graphs and statistical analyses were performed using GraphPad Prism 6 (GraphPad Software, Inc.). The mRNA expression datasets of leukemias were obtained from Oncomine. The Kaplan-Meier method was used to evaluate the association between OS and TRIB2 and draw the survival curve. Patients were separated into two groups using median gene expression, and the log-rank test was used to compare the differences between groups. Statistical analysis was performed using an appropriate analysis of variance (ANOVA) when more than two groups were compared. Tukey's post hoc test was used following ANOVA. Comparisons between the control and experimental groups were performed using the Student's t-test. For unpaired samples, unpaired t-tests were used. For paired datasets, paired t-test were used. $P<0.05$ was considered to indicate a statistically significant difference.

Results

TRIB2 promotes the proliferation of KG cells and increases the IC_{50} of IM. The IM resistance index of KG cells was 24.61 (Fig. 1A). The protein expression levels of TRIB2 in IM-resistant CML and CML specimens were compared using the Oncomine database. The results revealed that the expression level of TRIB2 was higher in IM-resistant specimens than in normal CML specimens (Fig. 1B). Subsequently, the expression of TRIB2 in cells was examined at the mRNA and protein levels and was found to be higher in KG cells than in K562 cells (Fig. 1C and D). KG cells proliferated faster

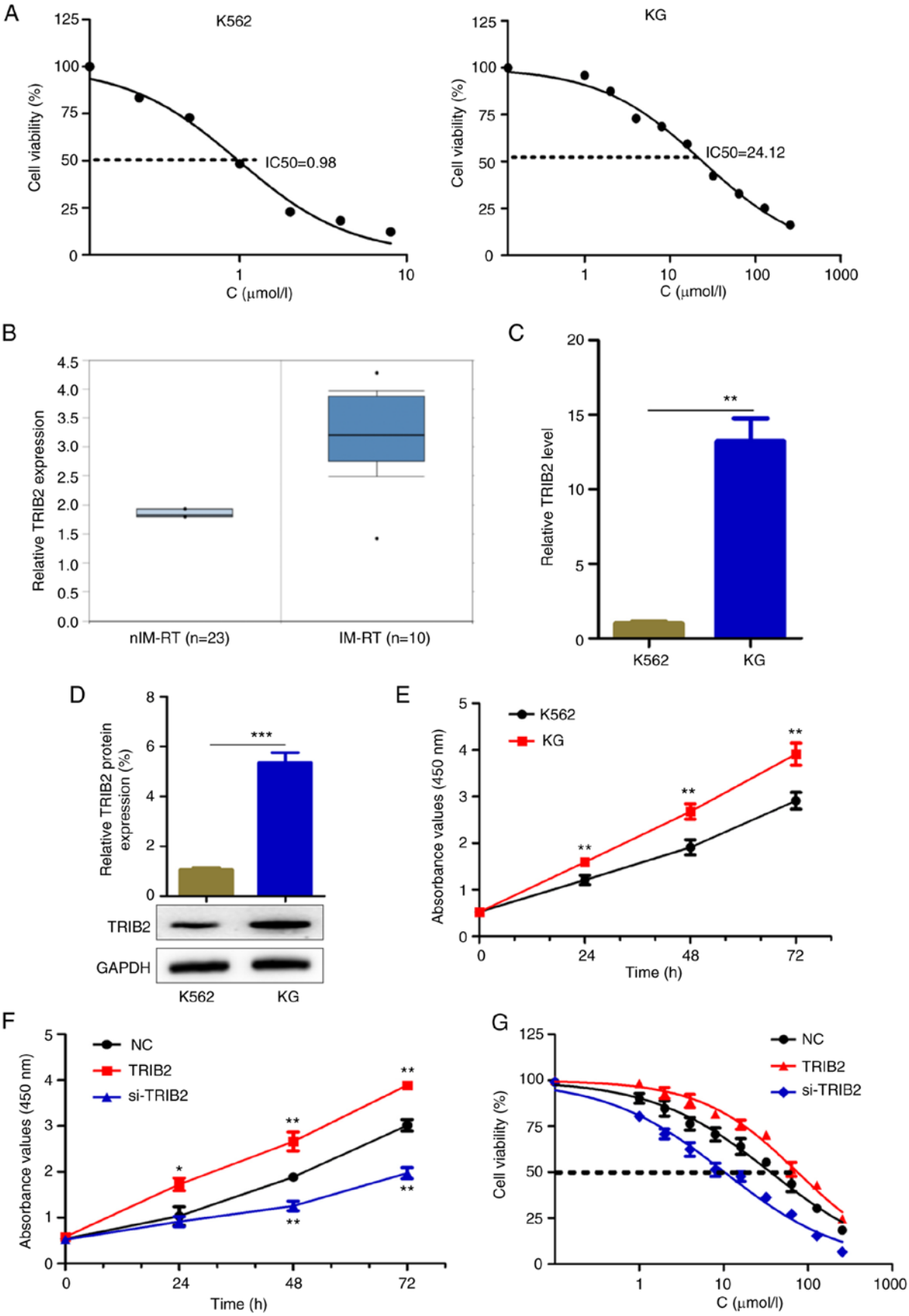

Figure 1. TRIB2 promotes the proliferation of KG cells and increases the IC_{50} of IM. (A) The IM resistance index of KG cells was 24.61. (B) TRIB2 was highly expressed in IM-resistant patients with chronic myeloid leukemia as identified from the Oncomine database. (C and D) TRIB2 was highly expressed in KG cells compared with K562 cells as detected by (C) RT-qPCR and (D) western blot analysis. (E) The proliferation rate of KG cells was found to be faster than that of K562 cells as revealed by CCK-8 assays. (F and G) TRIB2 promoted the (F) proliferation of KG cells and (G) increased the IC_{50} of IM as revealed by CCK-8 experiments. $^{*}P<0.05$, $^{**}P<0.01$ and $^{***}P<0.001$. TRIB2, tribbles pseudokinase 2; IM, imatinib; C, concentration; RT-qPCR, reverse transcription-quantitative PCR; CCK-8, Cell Counting Kit-8; si-, small interfering; NC, negative control.

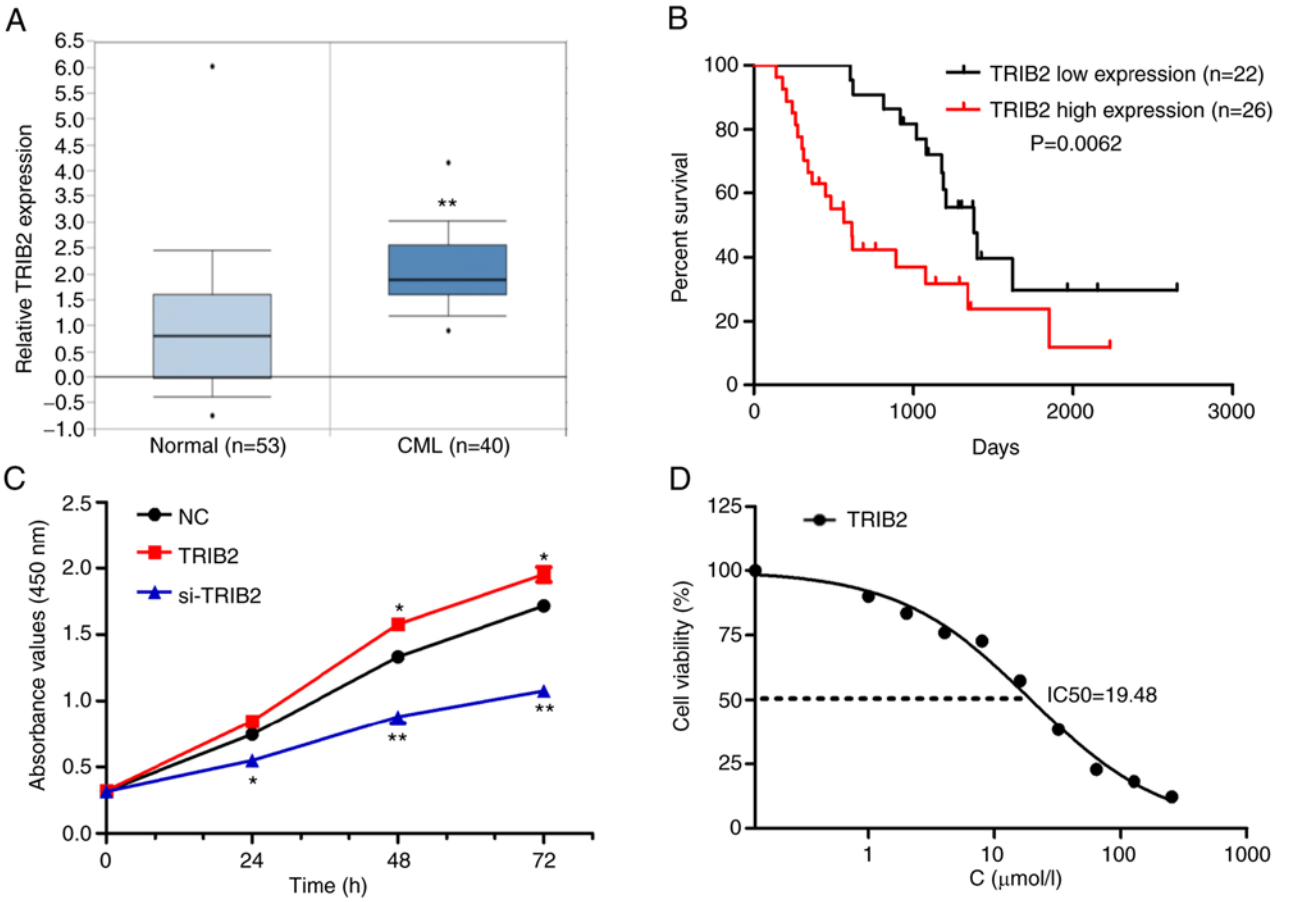

Figure 2. TRIB2 promotes K562 cell proliferation and increases IM resistance. (A) TRIB2 was highly expressed in CML patients compared with that in normal subjects as revealed from the Oncomine database analysis. (B) Kaplan-Meier plot of overall survival. CML patients with high expression of TRIB2 (Oncomine database) had worse survival. (C and D) TRIB2 promoted the (C) proliferation of K562 cells and (D) increased the IC_{50} value of IM as revealed by Cell Counting Kit-8 experiments. *P<0.05 and **P<0.01. TRIB2, tribbles pseudokinase 2; IM, imatinib; C, concentration; CML, chronic myeloid leukemia; si-, small interfering; NC, negative control.

than K562 cells, as evidenced CCK-8 assay (Fig. 1E), which suggested that TRIB2 might promote the growth of KG cells. To further investigate the role played by TRIB2 in KG cells, TRIB2 was successfully overexpressed or knocked down in KG cells, which was verified experimentally using RT-qPCR (Fig. S1A), Western blot (Fig. S1B) and fluorescence microscopy (Fig. S1C). TRIB2 was found to promote cell proliferation (Fig. 1F), and increase the IC_{50} of IM (Fig. 1G). Therefore, TRIB2 promotes proliferation of IM-resistant cells and increases the IC_{50} of IM in these cells.

TRIB2 promotes K562 cell proliferation and increases IM resistance. The Oncomine database showed that TRIB2 was highly expressed in patients with CML (Fig. 2A). Further analysis of CML datasets from the Oncomine database revealed that patients with high expression of TRIB2 experienced significantly worse overall survival (Fig. 2B). To further investigate the role played by TRIB2 in K562 cells, TRIB2 was successfully overexpressed or knocked down in K562 cells, which was verified using RT-qPCR (Fig. S1D), Western blot (Fig. S1E), and photographs by green fluorescence microscope (Fig. S1F). TRIB2 was found to promote cell proliferation (Fig. 2F), but also increased the IC_{50} of the cells (Fig. 2G). Therefore, TRIB2 promoted K562 cell proliferation and increased IM resistance.

TRIB2 promotes proliferation and IM resistance of KG cells in vivo. To investigate the role played by TRIB2 in leukemia-bearing mice after intravenous injection, a KG leukemia mice model was established (Fig. 3A). The TRIB2-related stable transgenic cell line was injected into the mice through the tail vein, and blood smear and count were used to confirm the successful modeling of leukemia model mice (Fig. 3B and C). It was found that TRIB2 could promote the proliferation of KG cells by a blood cell sorter (Fig. 3D). In addition, the TRIB2 overexpression group had worse survival in the model mice (Fig. 3E). The aforementioned experiments revealed that TRIB2 promoted the proliferation of KG cells within the model mice. The role of TRIB2 on KG tumor generation was further confirmed *in vivo* by transplanting tumors in mice. Plotting the growth curve indicated that the volume of tumor overexpressing TRIB2 showed a faster growth than the control group, whereas knockdown of TRIB2 revealed a slower growth (Fig. 3F and G). Overexpression of TRIB2 promoted tumors with high weight, whereas low-expression TRIB2 promoted tumors with low weight (Fig. 3H). Thus, these xenograft experiments demonstrated that TRIB2 can promote the proliferation of IM-resistant cells.

The relationship between TRIB2 and IM resistance was investigated using the Oncomine database to explore the drug

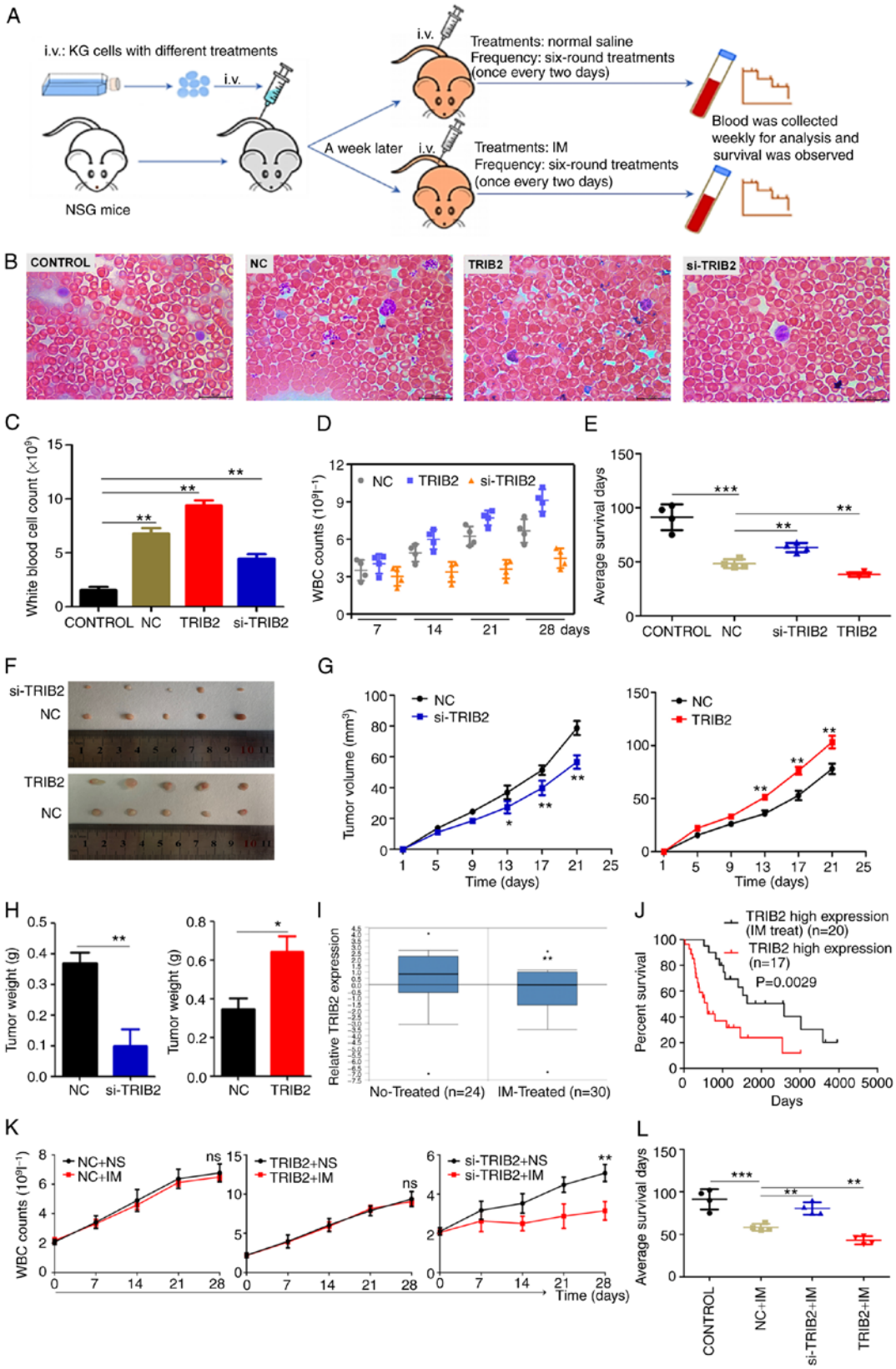

Figure 3. TRIB2 promotes the proliferation and IM resistance of KG cells *in vivo*. (A) Illustration of experimental design for assessing the effect of TRIB2 *in vivo*. (B and C) Successful modeling of chronic myeloid leukemia model mice was confirmed by blood counts and microscopic observation of blood smears (magnification, x1,000). (D) WBC counts of leukemia-bearing mice at different time points after various treatments. The number of WBC from mice overexpressing TRIB2 leukemia model grew at the fastest rate. (E) Compared with NC group, TRIB2 overexpression led to poor survival in the model mice, whereas TRIB2 knockdown resulted in improved survival. (F and G) In tumor-bearing nude mice, the volume of xenograft tumors overexpressing TRIB2 showed faster growth, while knockdown TRIB2 exhibited slower growth. (H) In tumor-bearing nude mice, overexpression TRIB2 promoted xenograft tumors with high weight, and TRIB2 knockdown promoted those with low weight. (I and J) Analysis of the Oncomine database showed decreased TRIB2 expression and improved survival after IM treatment. (K and L) si-TRIB2 increased the sensitivity of KG cells to IM in leukemia model mice, prolonging their survival. *P<0.05, **P<0.01 and ***P<0.001. i.v., intravenous; TRIB2, tribbles pseudokinase 2; IM, imatinib; WBC, white blood cell; si-, small interfering; NC, negative control.

Table II. Survival time and life extension rate of model mice.

Group	Average survival, days	Extension rate, %
Control	91.25±2.533	
TRIB2-NC	48.25±3.750	19.71
TRIB2-NC + IM	58.25±2.345	
si-TRIB2	63.25±3.473	27.17
si-TRIB2 + IM	80.50±2.598	
TRIB2	38.25±2.016	12.40
TRIB2 + IM	43.00±2.380	

n=4 in each group. TRIB2, tribbles pseudokinase 2; si, small interfering RNA; IM, imatinib; NC, negative control.

sensitivity of TRIB2 on KG cells *in vivo*. It was revealed that TRIB2 expression decreased after IM treatment and survival was improved (Fig. 3I and J). Cell proliferation was examined following IM treatment, and the results identified that there was no change in cell proliferation after overexpression of TRIB2. Both the NC group and si-TRIB2 group showed slower cell proliferation under IM treatment, and the si-TRIB2 group revealed the slowest cell proliferation. This indicated that knockdown of TRIB2 rendered KG cells more sensitive to IM (Fig. 3K). In agreement with database studies, IM was used to treat leukemia mice. It was found that drug treatment could prolong the survival time of mice in each group (Fig. 3L), but the life prolonging rate of the low-expression TRIB2 group was significantly higher than that of the high-expression TRIB2 group (Table II). This finding indicated that TRIB2 promoted proliferation and resistance to IM of KG cells *in vivo*.

TRIB2 regulates the expression of miR-33a-5p through the ERK/c-Fos signaling pathway. The aforementioned results indicated that TRIB2 can promote KG cell proliferation and enhance cell drug resistance. The mechanism by which TRIB2 exerts its effects was the focus of the next experiment. It was found that TRIB2 could downregulate the promoter activity of miR-33a-5p by dual-luciferase reporter assay, which was again further confirmed by RT-qPCR (Fig. 4A). Potential TFs that bind to the miR-33a-5p promoter were predicted via JASPAR and c-Fos was screened by prophase experiments to investigate the effect of TRIB2 on miR-33a-5p expression (Fig. 4B). The website prediction results were validated by ChIP assay, which demonstrated c-Fos as a TF for miR-33a-5p promoter (Fig. 4C). c-Fos was successfully transfected and overexpressed in KG and K562 cells (Fig. S1G-H). Subsequently, it was found that c-Fos inhibited miR-33a-5p expression and therefore played an inhibitory role in transcriptional effects (Fig. 4D). In addition, c-Fos was found to bind to TATA box binding protein (TBP) and suppress transcription (Fig. 4E). Notably, co-precipitation and immunoblotting experiments were performed to verify the inability of binding interaction between TRIB2 and c-Fos (Fig. 4F). Through further experiments, it was identified that the ERK signaling pathway could decrease miR-33a-5p promoter activity and then affect the expression of miR-33a-5p (Fig. 4G). The activation of the ERK signaling pathway can be regulated by TRIB2, which was confirmed experimentally by western blotting (Fig. 4H). Finally, the ERK pathway blocker U0126 and activator HNK were applied to the cells and detected the expression of related proteins. The results showed that UO126 inhibited and HNK increased ERK and c-Fos activity. It was further revealed that TRIB2 could activate the ERK pathway and then promote c-Fos expression (Fig. 4I-L). It was similarly concluded that TRIB2 could promote c-Fos expression by western blot analysis of transplanted tumors in nude mice from *in vivo* experiments (Fig. 4M). The aforementioned results suggested that TRIB2 regulated c-Fos expression through the ERK signaling pathway (Fig. 4N).

Specific site of action of c-Fos on the miR-33a-5p promoter. The presence of nine c-Fos possible binding sites on the miR-33a-5p promoter was predicted by JASPAR. To investigate which binding site specifically plays a role, by location of the nine binding sites, truncations of the miR-33a-5p promoter were made and constructed into a luciferase vector. A total of four segments of vectors were constructed -2000 ~+69 nt, -1575 ~+69 nt, -1124 ~+69 nt, and -534 ~+69 nt (Fig. 5A). The site of action was determined by the luciferase assay to be in the –534 to 1124 region (Fig. 5B and C). Two binding sites A (-958-965 nt) and B (-628-635 nt) were available for this fragment, and both sites were mutated (Fig. 5D). Further studies revealed that the luciferase activity was not altered when point mutation A was used, but it was altered when point mutation B was used (Fig. 5E-G). Description -958-965 nt is the specific site where c-Fos binds the miR-33a-5p promoter.

miR-33a-5p inhibits proliferation of KG cells and decreases IC_{50} by suppressing HMGA2 expression. The expression of miR-33a-5p in cells was detected by RT-qPCR to investigate the role played by miR-33a-5p in KG cells. The results showed that miR-33a-5p expression was decreased in KG cells compared with that in K562 cells (Fig. 6A). To verify the role of miR-33a-5p in drug-resistant cells, miR-33a-5p was successfully overexpressed and knocked down in cells, which was verified experimentally by RT-qPCR (Fig. S1I-J) and fluorescence microscopy (Fig. S1K). It was found that miR-33a-5p could inhibit KG cell proliferation and reduce IC_{50} (Fig. 6B and C). A KG cell xenograft mouse model was established to evaluate the role of miR-33a-5p in KG cell proliferation *in vivo*. Plotting the growth curve indicated that the volume of tumor knockdown miR-33a-5p showed a faster growth than the control group, whereas overexpression of miR-33a-5p showed a slower growth (Fig. 6D and E). The tumor weight was then measured and similar conclusions were reached (Fig. 6F and G). These results supported the conclusion that miR-33a-5p inhibits KG cell proliferation *in vivo*.

To investigate the mechanism of miR-33a-5p, the target gene of miR-33a-5p was predicted on the prediction website TargetScan. The results showed that there was a target binding site between miR-33a-5p and HMGA2 (Fig. 6H). Moreover, the target gene of miR-33a was detected by dual-luciferase reporter gene assay (Fig. 6I): miR-33a-5p could specifically bind to HMGA2, and HMGA2 was the target gene of miR-33a-5p. Further investigation by western blotting revealed that miR-33a-5p inhibited HMGA2 expression in KG cells (Fig. 6J). The same results were also found in nude mice xenografts (Fig. 6K and L). Through the aforementioned studies,

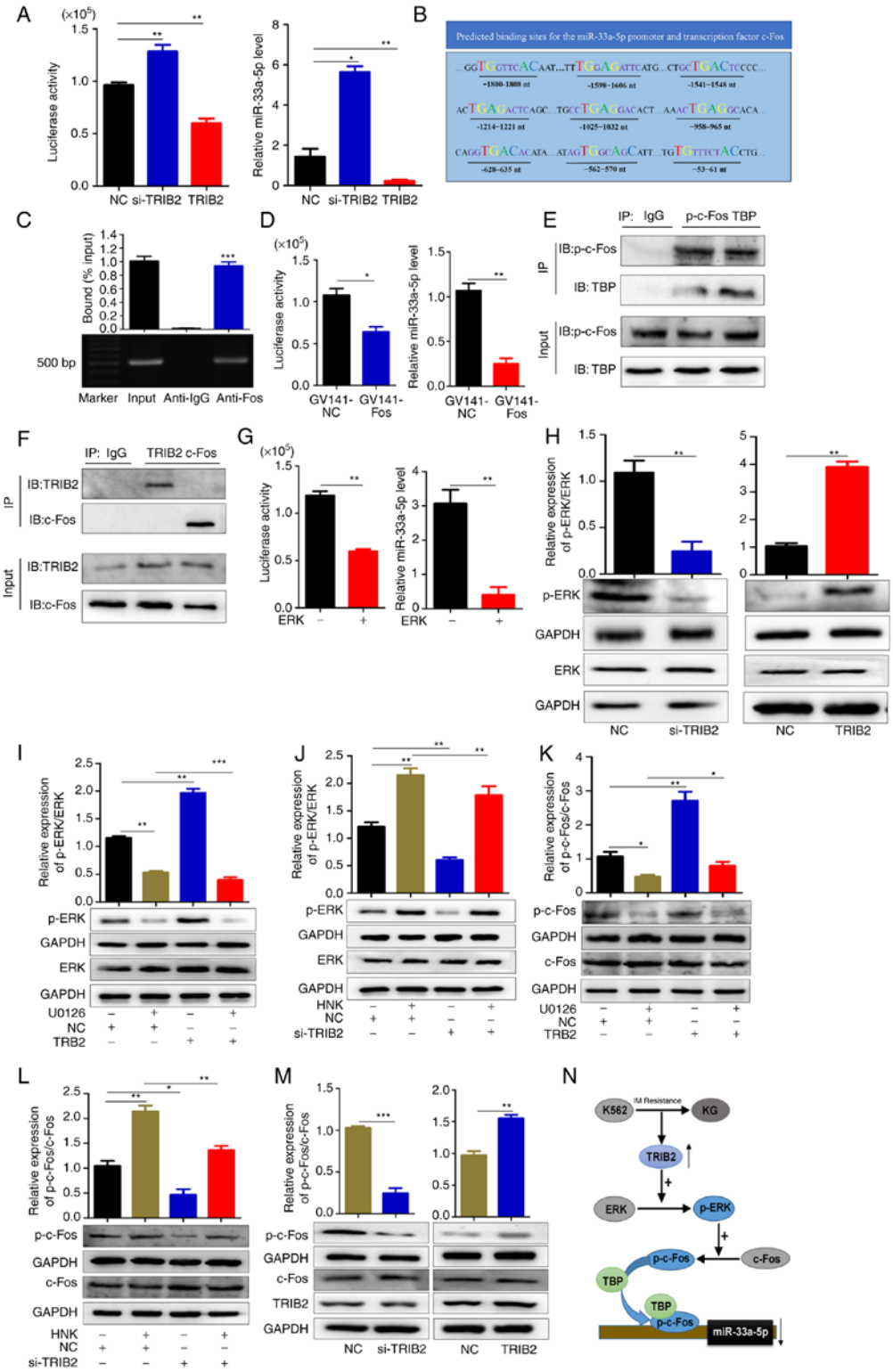

Figure 4. TRIB2 regulates the expression of miR-33a-5p through the ERK/c-Fos pathway in KG cells. (A) TRIB2 downregulated miR-33a-5p expression as revealed by luciferase activity assay and RT-qPCR. (B) Prediction of TF binding sites of miR-33a-5p promoter by JASPAR. (C) The ability of c-Fos as a TF and miR-33a-5p promoter region to bind was verified using chromatin immunoprecipitation experiments. (D) GV141-NC and GV141-Fos were transfected within KG cells, and the expression of miR-33a-5p after overexpression of c-Fos was detected by luciferase activity assay and RT-qPCR. (E) Co-IP verified that p-c-Fos and TBP were able to physically bind. (F) Co-IP verified that c-Fos and TRIB2 could not physically associate. (G) Overexpression of ERK decreased miR-33a-5p promoter activity, then downregulated miR-33a-5p expression. (H-J) TRIB2 promoted the phosphorylation of ERK, and this effect could be blocked by U0126. Knockdown of TRIB2 inhibited ERK phosphorylation, and this inhibitory effect could be relieved by HNK. TRIB2 can function through the ERK signaling pathway as revealed by western blotting. TRIB2 promoted the phosphorylation of ERK and this effect could be blocked by U0126. Knockdown of TRIB2 inhibited ERK phosphorylation and this inhibitory effect could be relieved by HNK. It was therefore hypothesized that TRIB2 might function through ERK signaling pathway. (K and L) TRIB2 could activate the ERK pathway and then promote c-Fos expression as revealed by western blotting. (M) The expression and phosphorylation levels of c-Fos and the expression of TRIB2 in mice xenografts were detected by western blotting. (N) Proposed model: Elevated TRIB2 expression in KG cells promoted phosphorylation of ERK, which in turn activated c-Fos expression, and c-Fos binding to TBP inhibited miR-33a-5p and transcriptionally repressed miR-33a-5p expression. *P<0.05, **P<0.01 and ***P<0.001. TRIB2, tribbles pseudokinase 2; miR, microRNA; RT-qPCR, reverse transcription-quantitative PCR; si-, small interfering; NC, negative control; TF, transcription factor; TBP, TATA box binding protein.

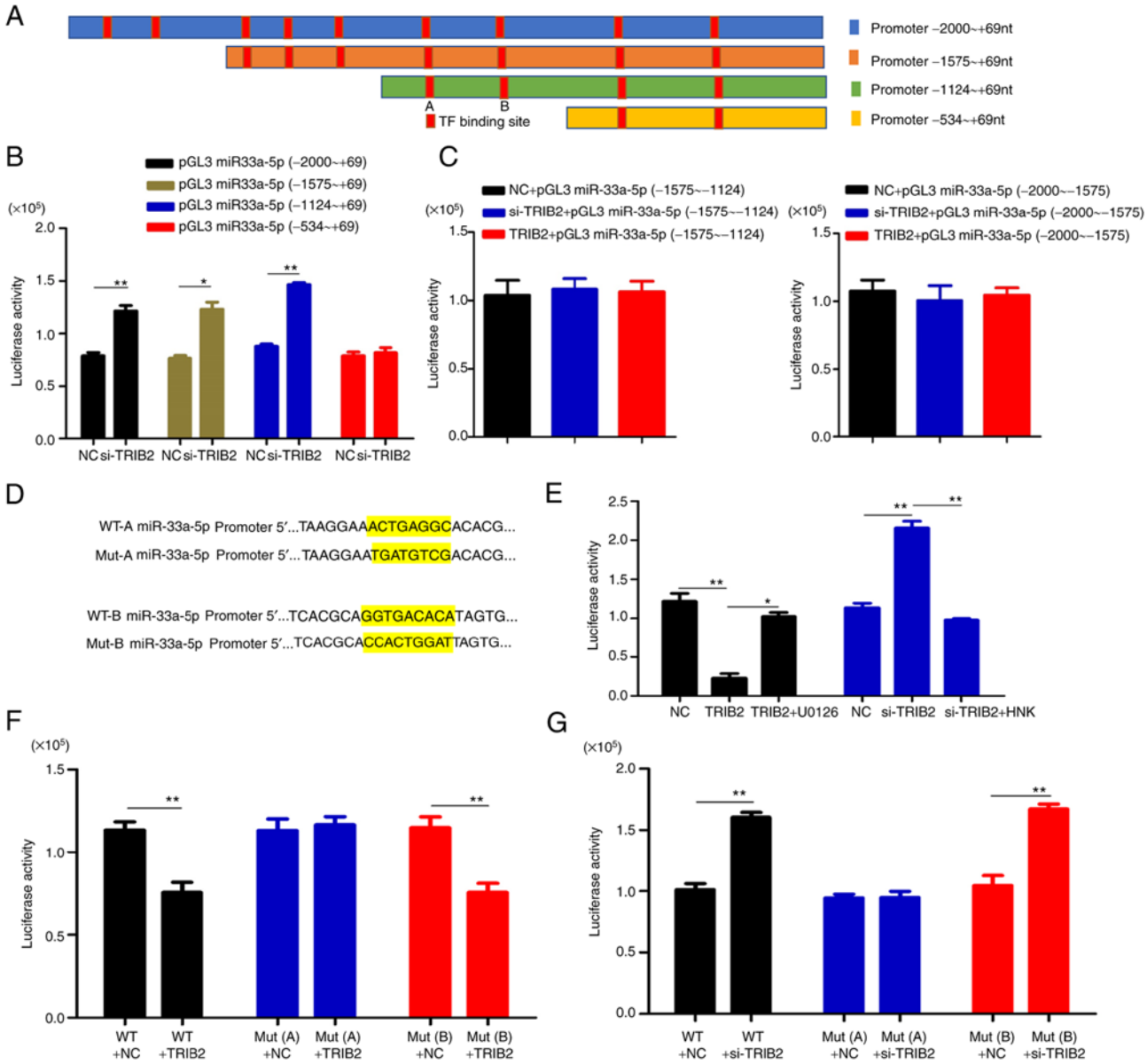

Figure 5. C-Fos in the binding site of miR-33a-5p. (A) Map of four miR-33a-5p promoter segment truncation carriers. (B and C) The fragment that exerted effect was verified by luciferase activity assay. (D) Binding site mutant sequences. (E) ERK pathway blockers and activators were used to verify the role of the ERK pathway in this process. (F) TRIB2 overexpression vector was used to determine the c-Fos-specific binding site to miR-33a-5p. (G) TRIB2 knockdown vector was used to determine the c-Fos-specific binding site to miR-33a-5p. All the aforementioned experiments were performed in KG cells. *P<0.05 and **P<0.01. miR, microRNA; TRIB2, pseudokinase 2; si-, small interfering; NC, negative control; WT, wild-type; Mut, mutant.

it was identified that miR-33a-5p can slow the proliferation of KG cells and increase the drug sensitivity of KG cells to IM by decreasing the expression of HMGA2.

Discussion

CML is a clinical hematological disease, and aberrant BCR-ABL fusion transcripts are a hallmark of the disease. Thus, IM is currently the first-line therapy to target the BCR-ABL fusion gene in CML (27). Although the application of IM is expected to overcome CML, a large body of clinical data indicated that patients develop acquired IM resistance as treatment duration increases (28,29). In response to the problem of drug resistance in leukemia, Zheng *et al* (30) found that chloroquine combined with IM overcame IM resistance through the MAPK/ERK pathway. S100A8 promotes drug resistance by promoting autophagy in leukemia cells, and S100A8 may be a novel target to improve leukemia drug resistance (31). At the same time ST6GAL1 had a reversal effect on multidrug resistance in human leukemia by regulating the PI3K/Akt pathway and the expression of P-gp and MRP1 (32). Research data treatment against leukemia drug resistance has focused on reversing drug resistance by targeting certain drug resistance proteins. However, whether these target proteins and their signaling pathways can be smoothly applied in the clinic and then exert clinical efficacy requires a long time of clinical experiments and exploration.

Tribbles are members of the pseudokinase family and were shown to regulate numerous cellular functions and were involved in various cellular processes including

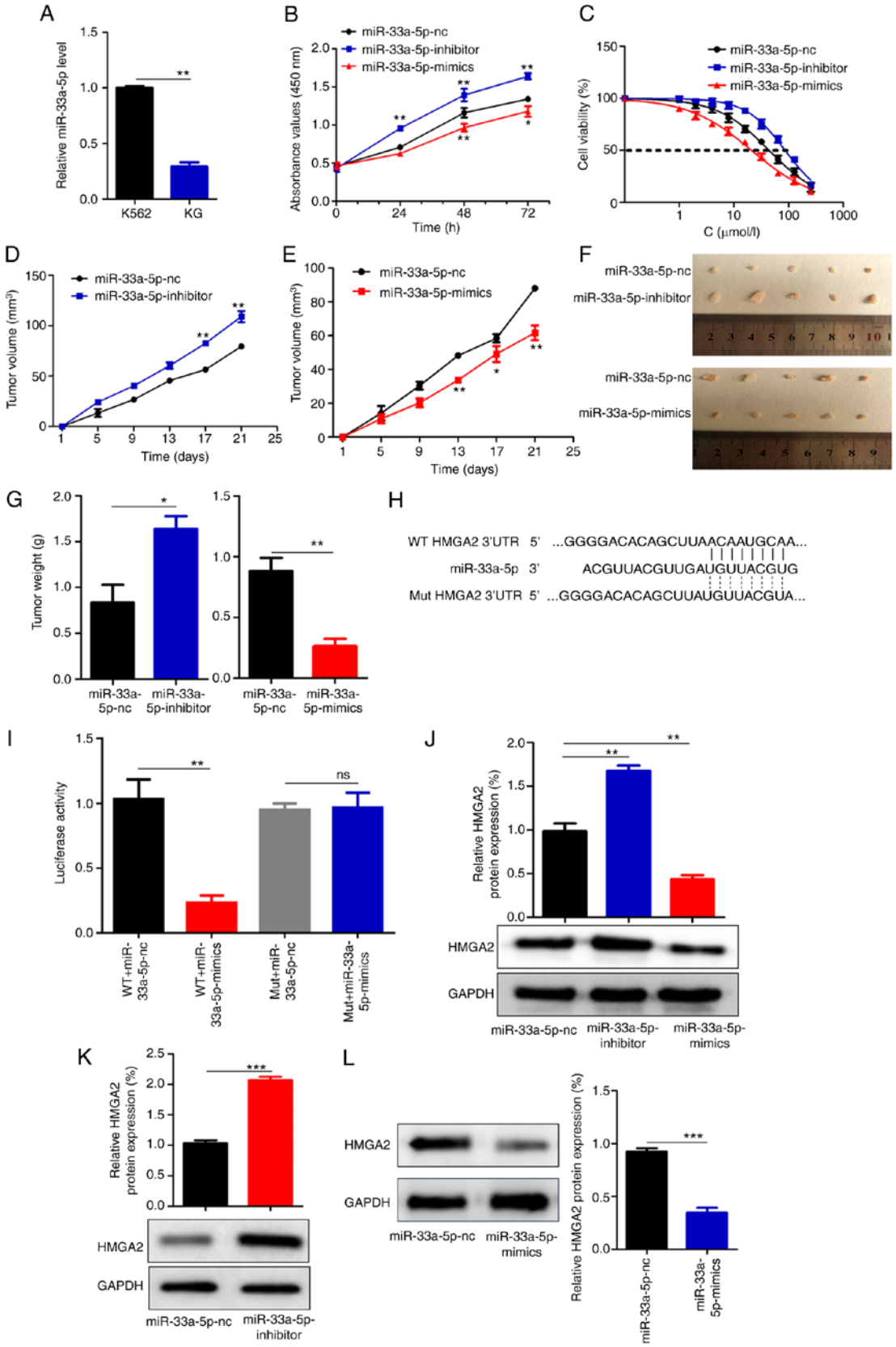

Figure 6. miR-33a-5p inhibits the proliferation of KG cells and decreases the IC_{50} of IM. (A) miR-33a-5p expression was decreased in KG cells compared with that in K562 cells. (B and C) miR-33a-5p inhibits KG cell proliferation and reduces the IC_{50} of IM. (D and E) In tumor bearing nude mice, the volume of xenograft tumor knockdown miR-33a-5p showed faster growth, while overexpression miR-33a-5p showed slower growth. (F and G) In tumor-bearing nude mice, transfection of the miR-33a-5p inhibitors increased tumor weight, whereas transfection of the miR-33a-5p reduced tumor weight. (H) The target binding sites between miR-33a-5p and HMGA2 were indicated by TargetScan prediction, a binding site was found at positions 262-269 of HMGA2. (I) The dual-luciferase assay showed that miR-33a-5p could specifically bind to HMGA2, and HMGA2 was the target gene of miR-33a-5p. (J) Western blot analysis showed that miR-33a-5p was able to downregulate HMGA2 expression levels in KG cells. (K and L) Western blotting showed that miR-33a-5p was able to downregulate HMGA2 expression levels in xenografts of nude mice. *P<0.05, **P<0.01 and ***P<0.001. miR, microRNA; NC, negative control; ns, no significance; WT, wild-type; Mut, mutant.

proliferation, drug resistance, metabolism and oncogenic transformation (33). In the present study, it was confirmed that TRIB2 promoted the proliferation of IM-resistant CML cells and increased their resistance to drugs. Furthermore, the role of TRIB2 *in vivo* was investigated to determine whether TRIB2 can serve as a potential target for the clinical treatment of IM resistance in CML. An IM-resistant CML model mice was established to mimic clinical resistant patients and it was experimentally confirmed that TRIB2 promoted the proliferation of IM-resistant cells and reduced drug sensitivity in model mice, while knockdown of TRIB2 reversed its drug resistance. Illustrating the important clinical role of TRIB2 in IM-resistant CML patients suggested that TRIB2 may be a novel target for the treatment of IM-resistant CML patients. TKIs are well known as kinase inhibitors that inhibit the activity of ABL tyrosine kinases (34,35). Similar to TKIs, whether a 'pseudokinase inhibitor' interferes with TRIB2 expression and then IM resistance in CML is unknown. Thus, addressing the question of clinical resistance is important. This aspect may require extensive basic research and clinical experiments for validation. Therefore, TRIB2 has potential as a resistance gene to treat IM resistance in CML.

A series of experiments was performed in the cell lines to further explore the oncogenic and drug sensitivity reducing roles played by TRIB2 in IM-resistant CML cells. It was found that TRIB2 acted by affecting miR-33a-5p. Accumulating evidence has indicated that miR-33a-5p and chemoresistance of tumors are associated and are downregulated in numerous different types of cancers to participate in the progression of tumors. For example, miR-33a-5p-based therapy may be a promising strategy for overgrowing the chemoresistance of TNBC (36). A possible mechanism of chemoresistance in liver cancer is downregulation of miR-33a-5p (37). In the present study, it was similarly found that miR-33a-5p could inhibit KG cells proliferation and enhance the sensitivity of KG cells to IM. The possible mechanism by which miR-33a-5p functions is through inhibiting HMGA2 expression. It has been reported that reducing HMGA2 expression levels can render tumor resistant cells more sensitive to the drug (38,39). Thus, miR-33a-5p has emerged as a key factor in the study of drug resistance in IM-resistant CML cells. ~20 clinical trials using miRNA and siRNA-based therapies have been initiated to date. Therapeutic miRNAs and siRNAs have moved from the laboratory to the clinic as the next generation of medicine. MiR-33a-5p-based therapies hold broad clinical promise for overcoming IM resistance in CML.

C-Fos, as an upstream factor of miR-33a-5p, regulates its expression and may provide a novel strategy to overcome IM resistance in CML clinically. It was experimentally confirmed that TRIB2 could affect the expression of miR-33a-5p by regulating c-Fos, which was a TF for miR-33a-5p. Given that the TF c-Fos can inhibit the activity of the miR-33a-5p promoter, it was hypothesized that c-Fos can physically bind to the TBP, which prevents the binding of TF IID to the promoter to inhibit transcription. The aforementioned hypothesis was verified by co-IP experiments and a literature review by Metz *et al* (40) that c-Fos can physically associate with TBP. PARP inhibitors (PARPi) were the first approved anticancer drugs, and they can improve the sensitivity of AML to chemotherapeutic agents as protein inhibitors (41). Similar to PARPi, inhibiting the expression of c-Fos may become a new direction and strategy for the clinical treatment of IM resistance in CML. In addition, Li *et al* (42) reported that the ERK/c-Fos signaling pathway plays a role in the proliferation and migration of colon cancer. This is consistent with the present study, in which it was also demonstrated that ERK/c-Fos signaling promoted IM resistance in KG cells.

In conclusion, TRIB2 can regulate c-Fos expression through the ERK signaling pathway and c-Fos, as a transcriptional suppressor of miR-33a-5p, could inhibit the transcription of miR-33a-5p. Thus, TRIB2 regulates the expression of miR-33a-5p through the ERK/c-Fos pathway to affect the IM-resistance of CML cells. Ultimately miR-33a-5p exerts its effect by suppressing HMGA2 expression. The present study is promising for the clinical treatment of IM resistance in CML and can broaden the ideas of clinical treatment of IM resistance, find improved clinical treatment strategies for IM resistance, and address the problem of clinical patient resistance. Due to the limitations of experiments at the cellular or animal level, there is still a certain distance from cellular and animal studies to clinical applications. Therefore, this needs to be addressed by future collaborative research efforts between clinicians and scientists.

Acknowledgements

Not applicable.

Funding

The present study was supported by The National Natural Science Foundation of China (grant nos. 81800169, 31371321 and 82002604), The Natural Science Foundation of Shandong (grant no. ZR2019MH022), The Support Plan For Youth Entrepreneurship and Technology of Colleges and Universities in Shandong (grant no. 2019KJK014), The Shandong Province Taishan Scholar Project (grant no. ts201712067) and The Yantai Science and Technology Committee (grant no. 2018XSCC051).

Availability of data and materials

The datasets used and/or analyzed during the current study are available from the corresponding author on reasonable request.

Authors' contributions

YS, YL and SX performed study concept and design. HS, YL and XW performed development of methodology and writing, review and revision of the manuscript. HS, RW, YY, XZ, SR, DL, GS and HC provided acquisition, analysis and interpretation of data and conducted statistical analysis. HS, SX and YS confirm the authenticity of all the raw data. All authors read and approved the final version of the manuscript.

Ethics approval and consent to participate

The animal experiments were reviewed and approved (approval no. 2019-11-06) by the ethics committee of Binzhou Medical University (Yantai, China).

Patient consent for publication

Not applicable.

Competing interests

The authors declare that they have no competing interests.

References

1. Luo Z, Gao M, Huang N, Wang X, Yang Z, Yang H, Huang Z and Feng W: Efficient disruption of bcr-abl gene by CRISPR RNA-guided FokI nucleases depresses the oncogenesis of chronic myeloid leukemia cells. J Exp Clin Cancer Res 38: 224, 2019.
2. Heaney NB, Pellicano F, Zhang B, Crawford L, Chu S, Kazmi SM, Allan EK, Jorgensen HG, Irvine AE, Bhatia R and Holyoake TL: Bortezomib induces apoptosis in primitive chronic myeloid leukemia cells including LTC-IC and NOD/SCID repopulating cells. Blood 115: 2241-2250, 2010.
3. Chen SH, Hsieh YY, Tzeng HE, Lin CY, Hsu KW, Chiang YS, Lin SM, Su MJ, Hsieh WS and Lee CH: ABL genomic editing sufficiently abolishes oncogenesis of human chronic myeloid leukemia cells in vitro and in vivo. Cancers (Basel) 12: 1399, 2020.
4. Tauer JT, Hofbauer LC, Jung R, Gerdes S, Glauche I, Erben RG and Suttorp M: Impact of long-term exposure to the tyrosine kinase inhibitor imatinib on the skeleton of growing rats. PLoS One 10: e0131192, 2015.
5. Cortes J, Hochhaus A, Hughes T and Kantarjian H: Front-line and salvage therapies with tyrosine kinase inhibitors and other treatments in chronic myeloid leukemia. J Clin Oncol 29: 524-531, 2011.
6. Wang XY, Zhang XH, Peng L, Liu Z, Yang YX, He ZX, Dang HW and Zhou SF: Bardoxolone methyl (CDDO-Me or RTA402) induces cell cycle arrest, apoptosis and autophagy via PI3K/Akt/mTOR and p38 MAPK/Erk1/2 signaling pathways in K562 cells. Am J Transl Res 9: 4652-4672, 2017.
7. Fan Z, Luo H, Zhou J, Wang F, Zhang W, Wang J, Li S, Lai Q, Xu Y, Wang G, *et al*: Checkpoint kinase1 inhibition and etoposide exhibit a strong synergistic anticancer effect on chronic myeloid leukemia cell line K562 by impairing homologous recombination DNA damage repair. Oncol Rep 44: 2152-2164, 2020.
8. Mayoral-Varo V, Jimenez L and Link W: The critical role of TRIB2 in cancer and therapy resistance. Cancers (Basel) 13: 2701, 2021.
9. Hou Z, Guo K, Sun X, Hu F, Chen Q, Luo X, Wang G, Hu J and Sun L: TRIB2 functions as novel oncogene in colorectal cancer by blocking cellular senescence through AP4/p21 signaling. Mol Cancer 17: 172, 2018.
10. Kim HS, Oh SH, Kim JH, Sohn WJ, Kim JY, Kim DH, Choi SU, Park KM, Ryoo ZY, Park TS and Lee S: TRIB2 regulates the differentiation of MLL-TET1 transduced myeloid progenitor cells. J Mol Med (Berl) 96: 1267-1277, 2018.
11. Liang Y, Yu D, Perez-Soler R, Klostergaard J and Zou Y: TRIB2 contributes to cisplatin resistance in small cell lung cancer. Oncotarget 8: 109596-109608, 2017.
12. Liu Q, Zhang W, Luo L, Han K, Liu R, Wei S and Guo X: Long noncoding RNA TUG1 regulates the progression of colorectal cancer through miR-542-3p/TRIB2 axis and Wnt/β-catenin pathway. Diagn Pathol 16: 47, 2021.
13. Link W: Tribbles breaking bad: TRIB2 suppresses FOXO and acts as an oncogenic protein in melanoma. Biochem Soc Trans 43: 1085-1088, 2015.
14. Wang J, Zuo J, Wahafu A, Wang MD, Li RC and Xie WF: Combined elevation of TRIB2 and MAP3K1 indicates poor prognosis and chemoresistance to temozolomide in glioblastoma. CNS Neurosci Ther 26: 297-308, 2020.
15. Hill R, Madureira PA, Ferreira B, Baptista I, Machado S, Colaco L, Dos Santos M, Liu N, Dopazo A, Ugurel S, *et al*: TRIB2 confers resistance to anti-cancer therapy by activating the serine/threonine protein kinase AKT. Nat Commun 8: 14687, 2017.
16. Huang HY, Lin YC, Li J, Huang KY, Shrestha S, Hong HC, Tang Y, Chen YG, Jin CN, Yu Y, *et al*: MiRTarBase 2020: Updates to the experimentally validated microRNA-target interaction database. Nucleic Acids Res 48(D1): D148-D154, 2020.
17. Ren D, Yang Q, Dai Y, Guo W, Du H, Song L and Peng X: Oncogenic miR-210-3p promotes prostate cancer cell EMT and bone metastasis via NF-κB signaling pathway. Mol Cancer 16: 117, 2017.
18. Li X, Strietz J, Bleilevens A, Stickeler E and Maurer J: Chemotherapeutic stress influences epithelial-mesenchymal transition and stemness in cancer stem cells of triple-negative breast cancer. Int J Mol Sci 21: 404, 2020.
19. Diaz-Martinez M, Benito-Jardon L, Alonso L, Koetz-Ploch L, Hernando E and Teixido J: MiR-204-5p and miR-211-5p contribute to BRAF inhibitor resistance in melanoma. Cancer Res 78: 1017-1030, 2018.
20. Yin J, Zeng A, Zhang Z, Shi Z, Yan W and You Y: Exosomal transfer of miR-1238 contributes to temozolomide-resistance in glioblastoma. EBioMedicine 42: 238-251, 2019.
21. Li Z, Zhou G, Tao F, Cao Y, Han W and Li Q: circ-ZUFSP regulates trophoblasts migration and invasion through sponging miR-203 to regulate STOX1 expression. Biochem Biophys Res Commun 531: 472-479, 2020.
22. Tu J, Zhao Z, Xu M, Chen M, Weng Q and Ji J: LINC00460 promotes hepatocellular carcinoma development through sponging miR-485-5p to up-regulate PAK1. Biomed Pharmacother 118: 109213, 2019.
23. Chen J, Chen J, Sun B, Wu J and Du C: ONECUT2 accelerates tumor proliferation through activating ROCK1 expression in gastric cancer. Cancer Manag Res 12: 6113-6121, 2020.
24. Racca AC, Prucca CG and Caputto BL: Fra-1 and c-Fos N-Terminal deletion mutants impair breast tumor cell proliferation by blocking lipid synthesis activation. Front Oncol 9: 544, 2019.
25. Lou Z, Lin W, Zhao H, Jiao X, Wang C, Zhao H, Liu L, Liu Y, Xie Q, Huang X, *et al*: Alkaline phosphatase downregulation promotes lung adenocarcinoma metastasis via the c-Myc/RhoA axis. Cancer Cell Int 21: 217, 2021.
26. Ban MJ, Byeon HK, Yang YJ, An S, Kim JW, Kim JH, Kim DH, Yang J, Kee H and Koh YW: Fibroblast growth factor receptor 3-mediated reactivation of ERK signaling promotes head and neck squamous cancer cell insensitivity to MEK inhibition. Cancer Sci 109: 3816-3825, 2018.
27. Guilhot F, Druker B, Larson RA, Gathmann I, So C, Waltzman R and O'Brien SG: High rates of durable response are achieved with imatinib after treatment with interferon alpha plus cytarabine: Results from the International randomized study of interferon and STI571 (IRIS) trial. Haematologica 94: 1669-1675, 2009.
28. Ciftci HI, Radwan MO, Ozturk SE, Ulusoy NG, Sozer E, Ellakwa ED, Ocak Z, Can M, Ali TFS, Abd-Alla IH, *et al*: Design, synthesis and biological evaluation of pentacyclic triterpene derivatives: Optimization of Anti-ABL kinase activity. Molecules 24: 3535, 2019.
29. Nardi V, Naveiras O, Azam M and Daley GQ: ICSBP-mediated immune protection against BCR-ABL-induced leukemia requires the CCL6 and CCL9 chemokines. Blood 113: 3813-3820, 2009.
30. Zheng S, Shu Y, Lu Y and Sun Y: Chloroquine Combined with imatinib overcomes imatinib resistance in gastrointestinal stromal tumors by inhibiting autophagy via the MAPK/ERK pathway. Onco Targets Ther 13: 6433-6441, 2020.
31. Yang M, Zeng P, Kang R, Yu Y, Yang L, Tang D and Cao L: S100A8 contributes to drug resistance by promoting autophagy in leukemia cells. PLoS One 9: e97242, 2014.
32. Ma H, Cheng L, Hao K, Li Y, Song X, Zhou H and Jia L: Reversal effect of ST6GAL 1 on multidrug resistance in human leukemia by regulating the PI3K/Akt pathway and the expression of P-gp and MRP1. PLoS One 9: e85113, 2014.
33. Rome KS, Stein SJ, Kurachi M, Petrovic J, Schwartz GW, Mack EA, Uljon S, Wu WW, DeHart AG, McClory SE, *et al*: Trib1 regulates T cell differentiation during chronic infection by restraining the effector program. J Exp Med 217: e20190888, 2020.
34. Pulte D, Jansen L and Brenner H: Changes in long term survival after diagnosis with common hematologic malignancies in the early 21st century. Blood Cancer J 10: 56, 2020.
35. Bernardi S, Malagola M, Zanaglio C, Polverelli N, Dereli Eke E, D'Adda M, Farina M, Bucelli C, Scaffidi L, Toffoletti E, *et al*: Digital PCR improves the quantitation of DMR and the selection of CML candidates to TKIs discontinuation. Cancer Med 8: 2041-2055, 2019.
36. Guan X, Gu S, Yuan M, Zheng X and Wu J: MicroRNA-33a-5p overexpression sensitizes triple-negative breast cancer to doxorubicin by inhibiting eIF5A2 and epithelial-mesenchymal transition. Oncol Lett 18: 5986-5994, 2019.
37. Meng W, Tai Y, Zhao H, Fu B, Zhang T, Liu W, Li H, Yang Y, Zhang Q, Feng Y and Chen G: Downregulation of miR-33a-5p in hepatocellular carcinoma: A possible mechanism for chemotherapy resistance. Med Sci Monit 23: 1295-1304, 2017.

38. Deng X, Kong F, Li S, Jiang H, Dong L, Xu X, Zhang X, Yuan H, Xu Y, Chu Y, *et al*: A KLF4/PiHL/EZH2/HMGA2 regulatory axis and its function in promoting oxaliplatin-resistance of colorectal cancer. Cell Death Dis 12: 485, 2021.
39. Han S, Han B, Li Z and Sun D: Downregulation of long noncoding RNA CRNDE suppresses drug resistance of liver cancer cells by increasing microRNA-33a expression and decreasing HMGA2 expression. Cell Cycle 18: 2524-2537, 2019.
40. Metz R, Bannister AJ, Sutherland JA, Hagemeier C, O'Rourke EC, Cook A, Bravo R and Kouzarides T: c-Fos-induced activation of a TATA-box-containing promoter involves direct contact with TATA-box-binding protein. Mol Cell Biol 14: 6021-6029, 1994.
41. Rose M, Burgess JT, O'Byrne K, Richard DJ and Bolderson E: PARP Inhibitors: Clinical relevance, mechanisms of action and tumor resistance. Front Cell Dev Biol 8: 564601, 2020.
42. Li T, Li Z, Wan H, Tang X, Wang H, Chai F, Zhang M and Wang B: Recurrence-associated long non-coding RNA LNAPPCC facilitates colon cancer progression via forming a positive feedback loop with PCDH7. Mol Ther Nucleic Acids 20: 545-557, 2020.